

EARLY EXPERIMENTAL RESULTS OF THROMBOLYSIS USING CONTROLLED RELEASE OF TISSUE PLASMINOGEN ACTIVATOR ENCAPSULATED BY PLGA/CS NANOPARTICLES DELIVERED BY PULSE 532 nm LASER

M. MAHMOODI ^{a,b}, M. E. KHOSROSHAHI ^{a*}, F. ATYABI ^c

^aLaser and Nanobiophotonics Lab, Biomaterial Group, Faculty of Biomedical Engineering, Amirkabir University of Technology, Tehran, Iran

^bIslamic Azad University of Yazd, Faculty of Eng., Material Group, Yazd, PO Box 89195/155 Iran

^cNovel Drug Delivery Systems Lab, Faculty of Pharmacy, Medical Sciences, University of Tehran, PO Box 14155-6451, Iran

The purpose of this study is to prepare cationic nanoparticles (NPs) by coating chitosan (CS) on the surface of PLGA NPs and evaluate the possibility of laser thrombolysis and photomechanical drug delivery in a blood clot using pulse 532 nm laser. *In vitro* tPA release showed a sustained release profile for three days. The mean particle size and encapsulation efficiency of tPA NPs were in the range of 280-360 nm and 46.7%±1.56, 50.8%±1.09, respectively. The encapsulation efficiency and the particles size were increased as a result of coating with CS. The release kinetic was evaluated by fitting the experimental data to two standard release equations. The results showed that the PLGA/CS NPs maintain the highest weight percentages of dissolved clot. Also, the thrombolysis process can be enhanced by delivering tPA into clot during laser ablation based on the photomechanical effect due to optical cavitation bubbles. Therefore, our studies could offer an alternative for currently existing method for acute myocardial infarction.

(Received March 14, 2011; Accepted May 3, 2011)

Keywords: Laser thrombolysis; Frequency doubled Nd:YAG; PLGA/CS Nanoparticles, Tissue Plasminogen Activator; Drug delivery

1. Introduction

Drug delivery systems are an area of study in which researchers from almost every scientific discipline can make a significant contribution [1]. Understanding the fate of drugs inside the human body is a high standard classical endeavor, where basic and mathematical analysis can be used to achieve an important practical end. No doubt the effectiveness of drug therapy is closely related to biophysics and physiology of drug movement through tissue. Therefore, drug delivery system requires an understanding of the characteristics of the system, the molecular mechanisms of drug transport and elimination, particularly at the site of delivery. In the last decade DDS have received much attention since they can significantly improve the therapeutic effects of the drug while minimizing its side effects. In chemical methods, cationic lipids, polymers and liposomes can be used as a drug carrier [2,3] while physical methods such as high voltage electric pulse [4], CW ultrasound [5], extra corporeal shock wave [6,7], laser induced shock wave [8] have been used as a driving force for drug delivery.

Laser thrombolysis is an interventional procedure to remove clot in occluded arteries using laser energy. It offers cost, recovery time, and safety advantages over bypass surgery, in which surgeons must replace arteries but laser thrombolysis are limited because they cannot

*Corresponding author: khosro@aut.ac.ir

completely clear thrombotic occlusions in arteries, typically leaving residual thrombus on the walls of the artery. A laser system capable of selectively targeting the clot is therefore desirable. This capability is offered by lasers emitting in the ultraviolet and visible regions, where the absorption by clot is much higher than that by artery. The principal chromophore of clot in the visible waveband is hemoglobin present in the red blood cells. Since higher absorption coefficients require less energy per unit area to achieve ablation, threshold for artery is higher than that for clot. Pulsed lasers operating in this waveband at radiant exposures between the thresholds for artery and clot can therefore selectively remove clot [9]. Photomechanical drug delivery is a technique for localized drug delivery using laser-induced hydrodynamic pressure following cavitation bubble expansion and collapse. Therefore, using photomechanical drug delivery to enhance laser thrombolysis by delivering tPA into clot [10].

CS is an amino poly saccharide (poly 1,4-D-glucoamine) coated NPs have been fabricated with muco-adhesion and enhanced permeability properties for nasal epithelium application [11]. CS is biocompatible, biodegradable and non-toxic polymer. Furthermore, CS promotes the enhancement of drug transport across the cell membrane [12] and has been extensively applied in drug delivery systems and tissue engineering [13-15]. Since, these NPs exhibit a positive potential in PBS solution due to protonization of its amine groups, and have been applied to deliver proteins or DNA [13,14]. Therefore, they may be preferentially chosen as potentially safe and useful cations carriers for gene delivery [16]. CS is a weak base and is insoluble in water and organic solvents, however, it is soluble in dilute aqueous acidic solution with $\text{pH} < 6.5$. Particle size, density, viscosity, degree of deacetylation, and molecular weight are important characteristics of CS which influence the properties of pharmaceutical formulations based on CS.

Pharmacology reperfusion therapy for acute myocardial infarction (AMI) and ischemic stroke characterized by ST-elevation in the electrocardiogram was incorporated into the armamentarium of clinicians over 18 years ago and has had an extraordinarily beneficial impact on outcome. A new tactic is to employ encapsulated fibrinolytic agents, whereby the lytic compound is sequestered in polymer microcapsules. Encapsulation has important effects, including acting as a shield to protect the drug from inactivation and increasing its half-life. Also, higher drug circulation in time allows the administration of a lower dosage, with decreased probability of side-effects. In addition, encapsulation may help to avoid bleeding complication by maintaining fibrinogen levels [17-20].

Plasminogen activators (PAs) such as streptokinase (SK), urokinase, tPA, and genetically engineered one- and two- chain versions of tPA and urokinase have been administered effectively by intravenous infusion over a wide range of dosages. All of these agents show similar incidences and rates of reperfusion and problem with bleeding complications [21,22]. tPA is a protein involved in the breakdown of blood clots. Specifically, it is a serine protease found on endothelial cells, the cells that line the blood vessels. As an enzyme, it catalyzes the conversion of plasminogen to plasmin, the major enzyme responsible for clot breakdown. Because it works on the clotting system, tPA is used in clinical medicine to treat only embolic or thrombolytic stroke. Its use is contraindicated in hemorrhagic stroke and head trauma. It may be manufactured by using recombinant biotechnology techniques. tPA created in this way may be referred to as recombinant tissue plasminogen activator or rtPA. It is used in diseases where blood clot is the prime issue, such as pulmonary embolism, myocardial infarction and stroke. The clinical benefits of administering PAs for thrombolytic therapy may be markedly improved by developing new methods to promote clot lysis with reduced side effects. In this regard, a drug delivery strategy, such as encapsulating PAs (SK) into liposomes or polymeric microspheres as drug carriers to increase the therapeutic efficacy of conventional thrombolytic therapy has been demonstrated *in vitro* and *in vivo* animal models [23-26].

Many groups have developed methods for producing PLGA microspheres by dissolving polymers in a solvent and precipitating it into a sphere, e.g., using solvent evaporation, solvent removal, spray-drying or coacervation processes [22, 27-30]. The double- emulsion (water-in-oil-in-water), solvent evaporation/extraction method is one typical method widely used for the preparation of PLGA microspheres loaded with hydrophilic drug such as therapeutic proteins.

Many parameters determine the drug release behavior from CS microspheres. These include concentration and molecular weight of the CS, the type and concentration of crosslinking

agent, variables like stirring speed, type of oil, additives, crosslinking process used, drug CS ratio, etc. Drug release study from CS microspheres has generally shown that the release of the drug decreases with an increase in molecular weight and concentration of CS [31]. Typically, these microspheres will give out a very large burst of drug release upon immersion into the release medium. This initial burst release, referred to as the percentage /amount of drug release after 24 h, depends on the immediate diffusion of hydrophilic drug from polymer matrix, and complicated its correlation with the effective drug loading [32-33].

In this study, tPA-encapsulated PLGA and PLGA/CS were fabricated and drug delivery has been characterized in terms of particle size, thermal analysis, encapsulation efficiency, drug release profiles, weight of digested clot (%), and laser thrombolysis and photomechanical drug delivery. The release kinetics was evaluated by fitting the experimental data to Higuchi and Riger-Peppas equations.

2. Experimental

2.1 PLGA-encapsulated tPA NPs

Nanoparticles were fabricated via the W/O/W double emulsion solvent evaporation surface coating method, as previously described [23]. Briefly, 3ml of de-ionized aqueous recombinant human tissue-type plasminogen activator solution (rtPA) (Actilyse, Boehringer Ingelheim Pharma KG, Germany) with albumin as an emulsifier were poured into dichloromethane solution (DCM) (Merck, Germany) containing PLGA (50:50, Resomer RG 504H, Mw 48000, Bohringer Ingelheim, Germany), and then emulsified using a probe ultrasonicator (UP400S, hielscher, Germany) at 4°C to form an W/O emulsion. The W/O suspension at 4°C was added to 1wt% of polyvinyl alcohol (PVA; Mw 22000, Merck), and emulsified using the same sonicator in a pulse mode several times to produce W/O/W emulsion. 0.5wt% of PVA was added to the emulsion which was mechanically stirred. The suspension was evaporated at an ambient pressure to remove the solvent from the emulsified suspensions. The suspension that contained PLGA-encapsulated tPA NPs was centrifuged (Sigma, 3K30, RCF 25568, speed 16500 with rotor 12150H, Germany) at 4°C to separate the NPs from the suspension. Then, the NPS dried at a freeze dryer (Chaist, Alpha 1-2 LD plus, Germany) for storage.

2.2 CS-coated PLGA-encapsulated tPA NPs

To prepare the CS solution (low molecular, 80-85% deacetylation, Merck) for this work, CS was dissolved in 1% acetic acid solution and similarly PLGA NPs was followed, except that 0.1wt% CS solution and 0.5wt% PVA solution were added, instead of PVA 0.5% solution, to the aforementioned W/O/W emulsion with continuously stirring.

2.3 Characterization and morphology of NPs

The size of NPs in aqueous solution was determined at 25°C using laser light scattering with zeta potential measurement (Zetasizer ZS, Malvern, UK). The zeta potential of various NPs in de-ionized water was determined using the same analyzer. The samples were prepared by suspending the freeze dried NPs in 5ml deionized water. Transmission electron microscopy (TEM, Philips CM 10, HT 100 k) was used to determine the shape and study surface morphology of the NPs. This was done by placing the solution of NPs on a 200 mesh size copper grid that had been coated with carbon. Then, 2 wt% phosphotangstic acide was used to stain the NPs on the copper grid. After the NPs were air-dried at room temperature, the morphology of the stained NPs was observed. The experiment were repeated three times and results were presented as means and standard deviations from the triplicate (n=3). Significance in data between different process variables was assessed using all data points obtained over multiple batches via student's t-test and one way ANOVA with post-test. P value <0.05 was considered significant.

2.4 FTIR spectroscopy

The fourier transform infrared spectroscopy (FTIR) absorption spectra of the PLGA and PLGA/CS NPs were obtained using an FTIR spectrum analyzer at 4cm^{-1} resolution (Nicolet, Magna-IR Spec. 550, USA). To identify CS in PLGA/CS NPs, 5mg of the NPs was mixed with KBr and then their spectra were obtained using the analyzer. The absorption spectra were recorded in the range $1000\text{-}4000\text{cm}^{-1}$.

2.5 AFM topographical analysis

The typical scanning probe microscopy (SPM) forces are mechanical contact force, Van der Waals force, capillary forces, electrostatic forces, magnetic force etc. AFM relies on the interaction between the specimen and a nanometric tip attached to a cantilever, which scans the sample surface. Individual particles, size information (length, width, and height) and other physical properties (such as morphology and surface texture) measures by AFM. A Dualscope/Rasterscope system (C26, DME, Denmark) was used for all imaging by AFM. The microscope was equipped with a scanner that had a maximum XY scan range of 50 by 50 μm and a Z range of 2.7 μm and was operated by means of a Scan Master (95-50E), a real-time closed-loop scanning control system that allows for the accurate measurement, repositioning, and zooming in on selected features. The images were acquired by using silicon nitride cantilevers with high-aspect-ratio conical silicon tips; the force constants were 0.1 N/m for contact-mode imaging. AFM was used to study the morphology of the PLGA and PLGA/CS NPs.

2.6 DSC analysis

The differential scanning calorimetry (DSC) (Mettler Toledo, DSC 823e, Switzerland) was used to analyze the effects of the coating and drug on the thermal properties of the PLGA and PLGA/CS NPs. The NPs were weighted in standard aluminum pans. DSC curves were obtained at heating rate of $5^\circ\text{C}/\text{min}$ and temperature range of $0\text{--}550^\circ\text{C}$. The heating chamber was continuously purged with nitrogen gas at a rate of 30 ml/min.

2.7 Measuring tPA concentration

Measuring tPA aqueous solution was analyzed using HPLC (BIO-TEK Kontorn Inst., Detector 535, Italy) equipped with a C_{18} column at 37°C . The quantity of tPA was determined from the absorption intensity at the wavelength 254 nm. The same method was employed to determine the encapsulation efficiency (EE*) and release profiles of PLGA and PLGA/CS encapsulated tPA NPs.

2.8 In vitro release studies

Encapsulation efficiency for tPA loaded NPs were determined by HPLC method. The unencapsulated tPA concentration in the emulsion suspension was determined using the HPLC method after the NPs had been centrifuged and collected. 7.5 mg of NPs was dissolved in dichloromethane (DCM) and then 2.5 ml of isotonic phosphate buffer solution (PBS, pH 7.4) was added to the solution to extract the tPA. The quantity of the collected tPA was determined using HPLC. 30 mg dried tPA loaded NPs was suspended in 25 ml PBS with 1wt% sodium azide which were shaken at 70 rpm at 37°C ; 1ml of the dissolution was periodically drawn out to analyze tPA by the HPLC. The PBS with sodium azide was replaced equal volumes of fresh medium. The experiment was performed for a week.

2.9 Mathematical analysis of the drug release

In order to study tPA release mechanism from the PLGA NPs and PLGA/CS NPs, 2 models can be considered to fit the experimental data. Model 1 is based on the Higuchi equation

which describes the Fickian diffusion of drug [34]. Higuchi is the first to derive an equation to describe the release of a drug from a polymer as the square root of a time-dependent process based on Fickian diffusion (Eq. 1).

$$\frac{M_t}{M_0} = Q_t = \sqrt{2DS\varepsilon(A - 0.5S\varepsilon)} \times \sqrt{t} = K_H \sqrt{t} \quad (1)$$

Where,

$$K_H = \frac{X}{\sqrt{t_X}} \quad (2)$$

Where, Q_t is the amount of drug released in time (t), D is the diffusion coefficient, S is the solubility of drug in the dissolution medium, ε is the porosity, A is the drug content per cubic centimeter of polymer, and k_H is the release rate constant for the Higuchi model. Percentage drug released at the t_X is $X\%$ (Eq.2). For example, for an ideal t_{100} hour release profile (where t_{100} is the time required for 100% drug release), k_H is equal to $\frac{100}{\sqrt{t_{100}}}$ [35]. Model 2 is described by the Riger-Peppas equation (Eq.3) [36].

$$\frac{M_t}{M_{\infty}} = Kt^n \quad (3)$$

Where, M_t/M_{∞} is the fractional drug release, t is the release time and n is the diffusional exponent that can be related to the drug transport mechanism. When $n=0.5$, the drug release mechanism is Fickian diffusion, when $n=1$, occurs zero-order release. When the value of n is between 0.5 and 1, anomalous (non-Fickian) is observed. These mathematical models are valid only for the first 60% drug release.

2.10 Clot preparation

Venous blood was repeatedly collected from a healthy volunteer and anticoagulated into 5 ml glass tubes (inner diameter 13 mm) containing 0.5 ml of 105 mmol l⁻¹ sodium citrate. Aliquots of 1 ml of anticoagulated blood were recalcified with 100 μ l of 100 mmol l⁻¹ calcium chloride in a glass tube. The tubes were incubated for 2 hr at 37 °C in a water bath and then clots were removed from the tube and being washed with 154 mmol l⁻¹ sodium chloride. This method described by Cintas et al. allowed us to prepare whole blood clots with a good reproducibility in size and weight [37].

Clots were weighted before and after experiment. The mean weight of clots was measured prior to experiment as follow: 459.3 mg in the case of tPA only, 259.3 mg with PLGA NPs, and 228.4 mg with PLGA/CS. In the next step, NPs and tPA solution were added to clots separately and were placed in the occlusive tubes filled with PBS buffer. The tubes were then sealed and shaken at 70 rpm and 37 °C. The thrombus dissolution was monitored using a fast digital CCD camera (Panasonic Super Dynamic WV-CP450) connected to an optical microscope (Prior-UK). Thrombolysis was expressed as the relative reduction in clot weight (%) and the weight percentage of dissolved clot defined by equation.

$$\text{Weight of digested clot \%} = (\text{Weight of clot at the start}) - (\text{Weight of residual clot}) / (\text{Weight of clot at the start}) \quad (4)$$

2.11 Optical set up

Drug delivery experiments were performed by using a frequency-doubled Nd:YAG laser (532 nm) with 10 ns pulse duration. As it can be seen in Fig.1 the output of the laser was focused

by a 500 μm spot size at the surface of clot. Clot removal measurements were made by exposing the sample to a predetermined number of pulses, n , at pulse repetition frequency of 2Hz and the weight of clot loss was measured before and after each experiment. The laser beam scanned the entire clot surface at 2.33 mms^{-1} and number of scans of 2 ($N_s=2$), see Fig.2.

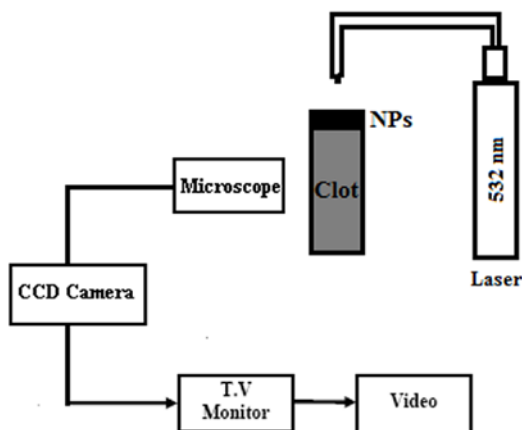


Fig.1. The experimental set up.

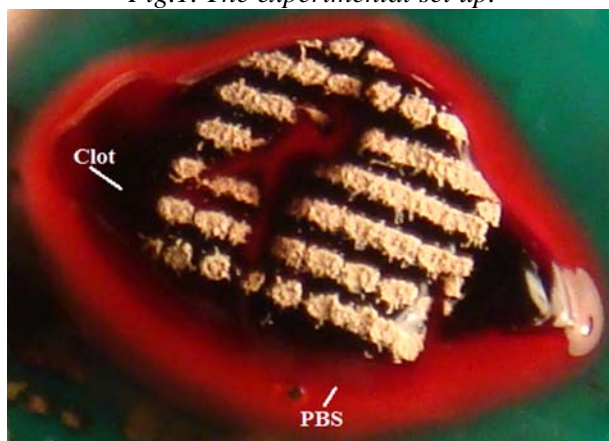


Fig.2. The scanned clot surface with laser at $N_s=2$.

3. Results

3.1 Characterizations of PLGA and PLGA/CS NPs

The spherical shape and the shell layer of the PLGA/CS NPs are shown by TEM micrographs (Fig.3). TEM micrographs of tPA encapsulated PLGA and PLGA/CS NPs show that they were spherical with solid cores. The main component of the shell layer of NPs in Fig 3b is CS. This micrographs are shown size of the tPA encapsulated PLGA/CS NPs is larger than PLGA NPs (Table 1). The hydrodynamic diameter of CS coated PLGA NPs increases gradually with initial CS concentration.

Table 1. The particle size, zeta potential and encapsulation efficiency of the nanoparticles (The data presented mean \pm SD with $n=3$).

Sample	Size (nm)	Zeta potential (mv)	PDI	EE*
tPA-PLGA NPs	282 ± 4.96	-8.92 ± 0.51	0.192	46.7 ± 1.56
tPA-PLGA/CS NPs	356 ± 2.94	$+5.95 \pm 0.17$	0.334	50.8 ± 1.09

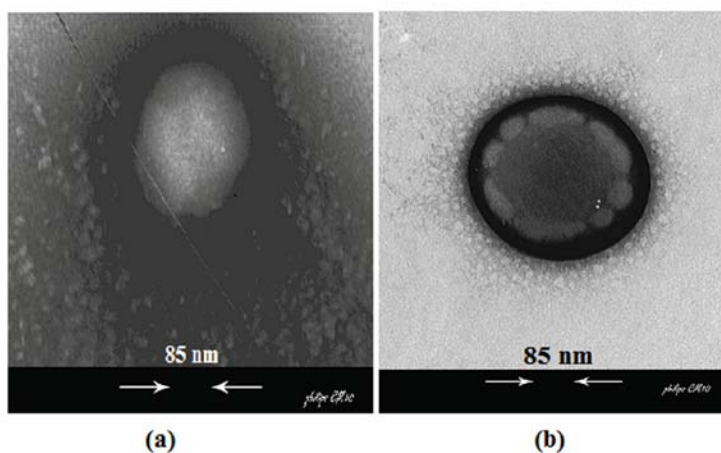


Fig. 3. TEM micrographs a) tPA -PLGA NPs, and b) tPA-PLGA/CS NPs.

Figure 4 shows 2D and 3D images of tPA encapsulated PLGA and PLGA/CS NPs. AFM images show their spherical shape and acceptable dispersion.

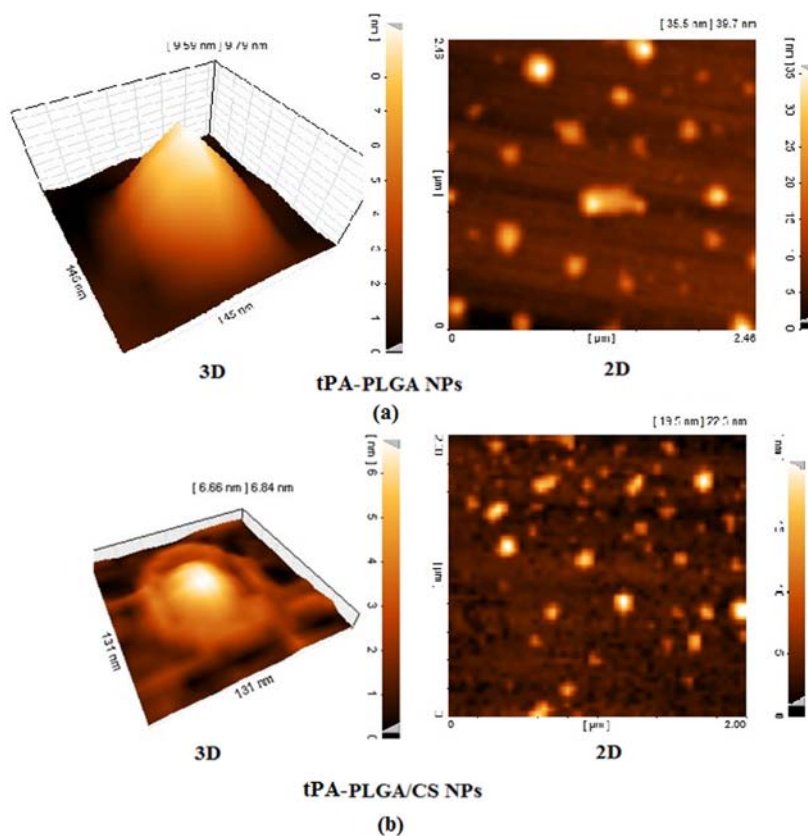


Fig.4. 2D and 3D AFM images of a) tPA -PLGA NPs, and b) tPA-PLGA/CS NPs.

The positive zeta potential (Table 1) and FTIR spectroscopy of CS coated PLGA NPs confirmed the presence of CS on PLGA NPs. Figure 5 illustrates a comparison between the FTIR spectra of CS, PLGA and PLGA/CS NPs. FTIR measurements results confirmed the presence of the CS on the surface PLGA/CS NPs. The characteristic absorption bands of amine group (NH) and OH, NH_3^+ , CH, CN at CS at 3431, 2923, 2853 and 1629 cm^{-1} respectively were observed. The peaks at 1095, 1184, and 1759 cm^{-1} and peaks around 3000 cm^{-1} are attributed to PLGA. The

strong peak at 1759 cm^{-1} is due to the C=O stretch. The peaks at 3431 cm^{-1} corresponds to stretching and libational modes of hydroxyl.

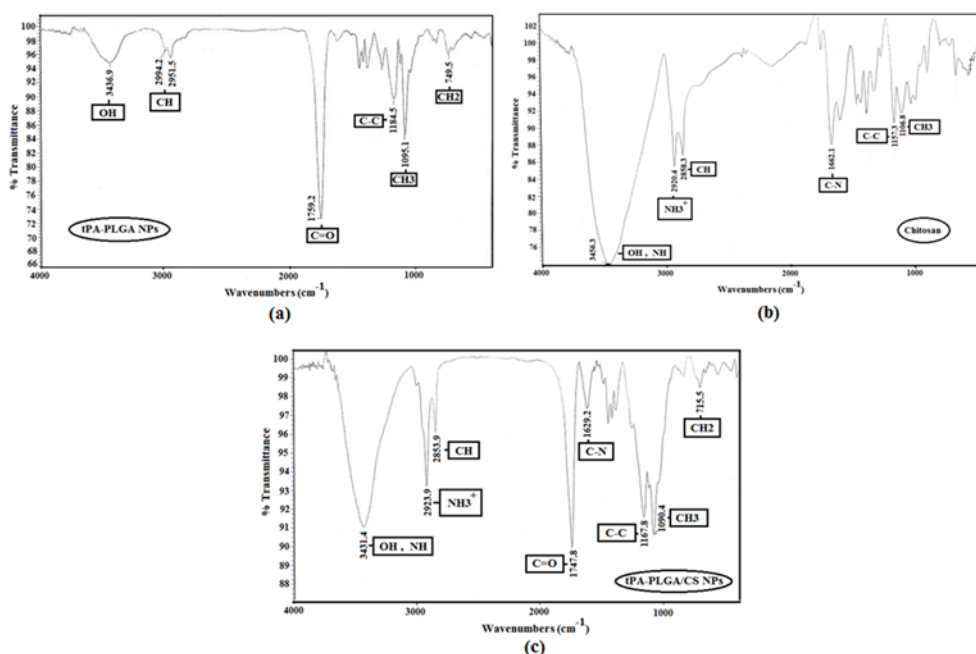


Fig.5. FTIR spectroscopy for a) tPA-PLGA NPs, b) CS, and c) tPA-PLGA/CS NPs.

3.2 Thermal analysis

Figure 6 illustrates the comparison between the DSC curve for PLGA and PLGA/CS NPs and provides a qualitative and quantitative information about the physical state of drug in NPs and in the control samples, i.e. the pure PLGA, the pure CS, the mixture of PLGA and CS and tPA. The pure tPA (Fig.6a) shows an endothermic peak that corresponds to the glass transition (T_g) at 110°C . After T_g , two peaks are observed due to the thermal decomposition of the drug, with maximum temperatures around 165 and 390°C . The pure PLGA exhibit an endothermic event (55°C) referring to the relaxation peak that follow T_g (Fig.6b). No melting point was observed, because PLGA appears amorphous in nature. The thermal stability of PLGA is until 25°C and the thermal decomposition has begun at approximately 35°C . The DSC curve of CS (Fig.6c) shows an endothermic peak (160°C) referring to T_g . The onset of thermal degradation of the CS is observed at 270°C . The thermal degradation in nitrogen is exothermic, and corresponding is observed at 300°C . The curve of CS shows that the polymer presents thermal stability until 250°C .

Figure 6d illustrates the mixture of PLGA and CS curve. The curve shows two endothermic peak that referring to T_g of the PLGA and CS. The thermal degradation of the mixture of PLGA and CS is observed at 250°C thermal decomposition begins approximately at the same temperature as the pure PLGA and CS.

The DSC curve of PLGA NPs (Fig.6e) corresponds to the relaxation enthalpy of PLGA (55°C). It can be observed that the nanoencapsulation process did not affect the polymer structure because the pure PLGA presented the same value for relaxation enthalpy. The thermal decomposition of PLGA NPs begins approximately at 285°C . Figure 6f shows two endothermic peaks of PLGA/CS NPs that correspond to T_g of PLGA (55°C) and thermal degradation of the CS (275°C).

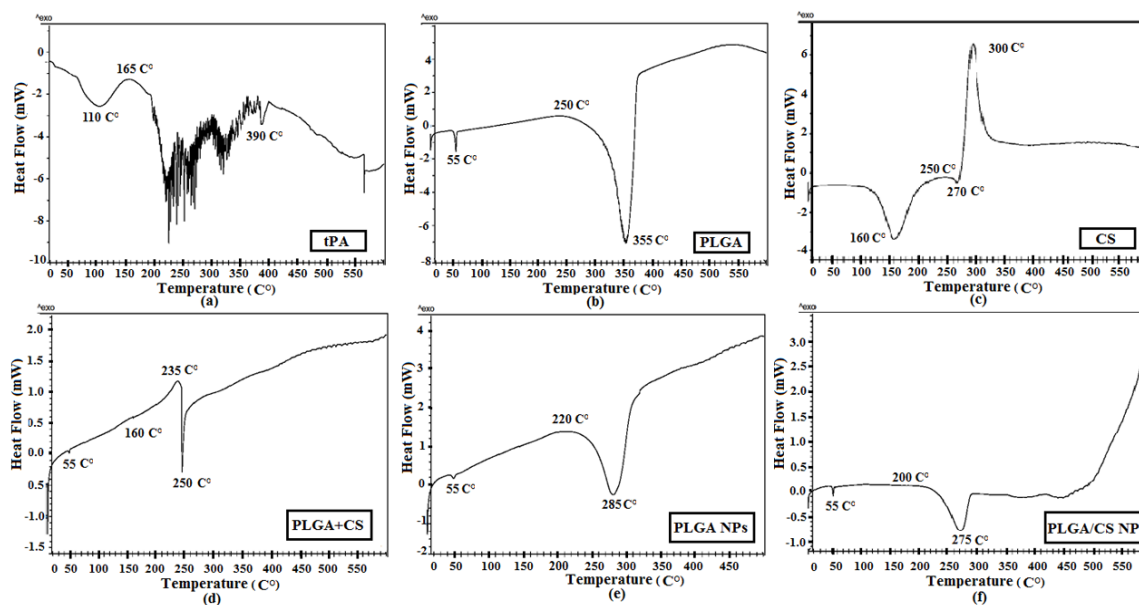


Fig. 6. DSC curves for a) tPA, b) PLGA, c) CS, d) the mixture of PLGA and CS, e) tPA-PLGA NPs, and f) tPA-PLGA/CS NPs.

3.3 tPA release from NPs

The EE^* of tPA encapsulated PLGA and PLGA/CS NPs are found to be $46.7\% \pm 1.56$, $50.8\% \pm 1.09$, respectively (Fig.7). Effect of coating with CS on loading efficiency might be caused by an ionic interaction between tPA and CS and prevented leakage of tPA from emulsion droplet during evaporation process.

Drug release from NPs involves three different stages: the first stage is an initial burst followed by drug diffusion, the second stage is governed by swelling of the polymer by inward diffusion of water during which the drug is dissolved and can diffuse out. The third stage is characterized by the erosion phase, in which polymer degradation occurs [38]. Initially, high release rate was observed due to the dissolution of surface adhered drug. The drug release of PLGA and PLGA/CS NPs were monitored during the first hour which accounted for 11% and 7.8 % respectively. After the initial release, it continued significantly for 2 days where 55% and 65% of tPA for PLGA and PLGA /CS was released respectively (Fig.8).

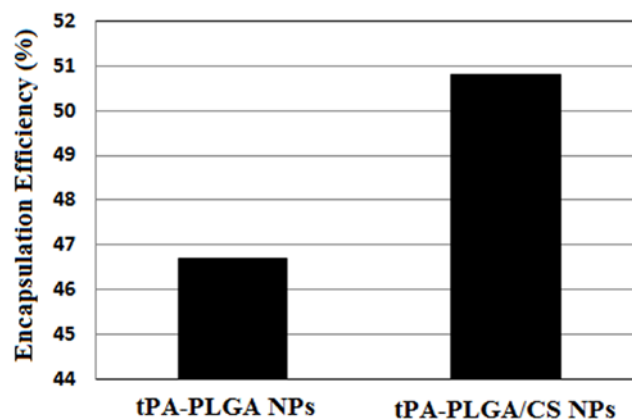


Fig.7. The EE^* of tPA- PLGA and tPA- PLGA/CS NPs.

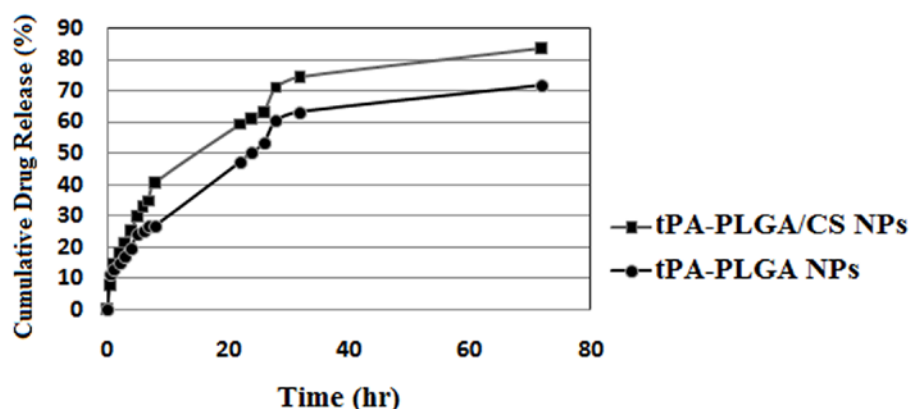


Fig.8. The cumulative release profiles of tPA- PLGA and tPA-PLGA/CS NPs.

3.4 Evaluation of release kinetic

The release kinetic was evaluated by fitting the experimental data to standard release equations (Riger-Peppas and Higuchi equation) (Eq.1 and Eq. 3). From the analysis of the first phase (<10% of drug released) and the last phase (>65% of drug released), can be deduced that Higuchi square-root of time model ($R^2 > 0.99$) (Fig.9) and Riger-Peppas equations ($R^2 > 0.99$) (Fig.10) for PLGA/CS NPs (Table 2). The drug release mechanism is non-Fickian diffusion ($n > 0.5$). The best fit was obtained for both models.

Table 2. The release parameters calculated by Higuchi and Riger-Peppas equations.

Sample	Riger-Peppas equation			Higuchi equation		
	R^2	n	K	R^2	K_H	K_H theory
tPA-PLGA NPs	0.9911	0.5286	12.80	0.9829	10.627	11.16
tPA-PLGA/CS NPs	0.9917	0.5038	9.63	0.9925	12.868	13.2

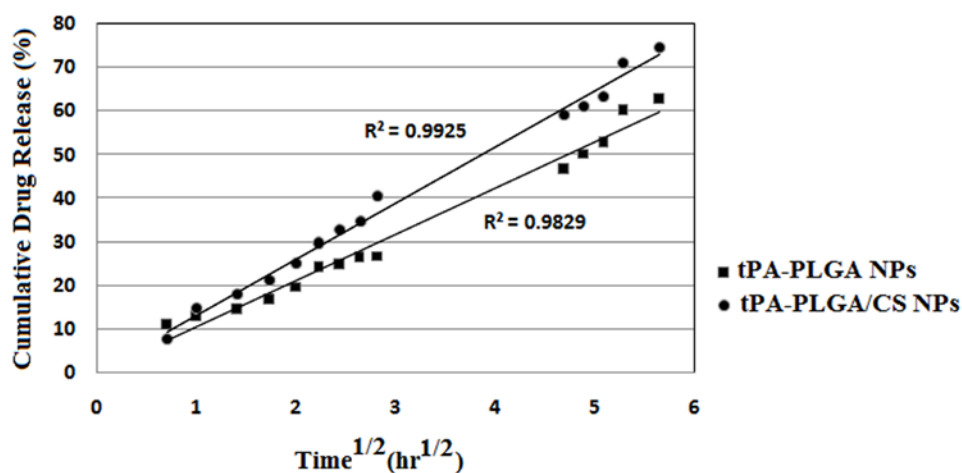


Fig.9. Drug release profiles from tPA-PLGA NPs and tPA-PLGA/CS NPs in PBS at pH 7.4 predicted by Higuchi equation.

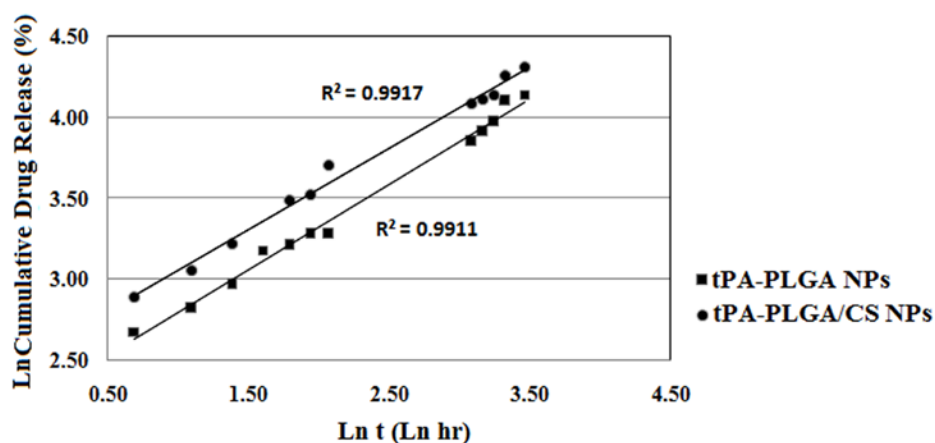


Fig.10. Drug release profiles from tPA-PLGA NPs and tPA-PLGA/CS NPs predicted by Riger-Peppas equation.

3.5 Thrombolysis of tPA-NPs

The thrombolysis of clots in an occlusive tube was examined by adding tPA only, PLGA NPs and PLGA/CS NPs into PBS solution. Thrombus weight reduction in each group is summarized in Table 3. The highest digested clot was obtained with PLGA/CS NPs (21.6%) while with tPA only the lowest (8.05%), suggesting the effect and important of the interaction between the CS and blood clot (Fig.11). Therefore, PLGA/CS NPs could serve as an effective vehicle for local delivery of tPA in an attempt to alleviate the systemic side effects of the drug and to enhance its efficacy in thrombolytic therapy.

Table 3. The weight of digested clots percent after exposure to NPs (after 1hr).

Sample	Initial weight (mg)	Final weight (mg) after exposure to NPs	Weight of digested clot (%)
tPA only	459.3	422.3	8.05
tPA-PLGA NPs	259.3	219	15.54
tPA-PLGA/CS NPs	228.4	179	21.62

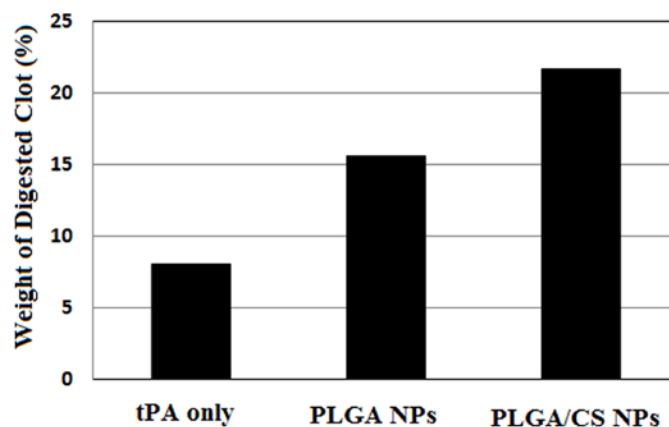


Fig.11. Plot of thrombolysis and weight of digested clots percent after exposure to NPs (after 1hr).

3.6 Laser thrombolysis and photomechanical drug delivery

Laser induced thrombolysis by photomechanically driven NPs investigated at room temperature. Mean weight of clots before laser exposure was 100 mg in group I: tPA only, 299.3 mg in group II: PLGA NPs, and 316.2 mg in group III: PLGA/CS NPs. As it can be seen from the Fig.12 the total weight loss (Eq.5) increases with increasing the fluence. However, it behaves linearly up to 70 Jcm^{-2} there on wards the curve shows a nonlinear behavior. A maximum weight loss of 69 mg is achieved at 135 Jcm^{-2} .

$$\text{Total weight loss} = (\text{Weight of clot at the start}) - (\text{Weight of residual clot}) \quad (5)$$

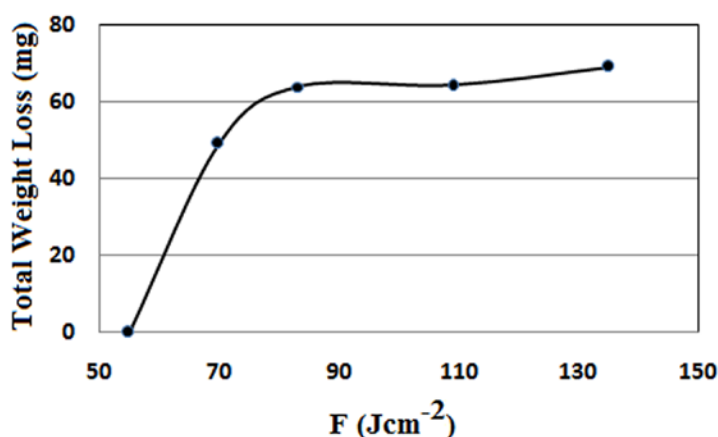


Fig.12. The total weight loss of clot versus fluence.

Weight reduction of clots in each group after laser exposure is summarized in Table 4. The next step was to study the percent of clot dissolution under the influence of tPA release at different times. The rate of thrombolysis obtained for PLGA/CS NPs was highest at different times (Fig.13). Results presented in this study demonstrated the possibility of using photomechanical drug delivery to enhance the thrombolysis process by delivering nanoparticles into clot during the laser thrombolysis procedure or possibly to remove the clot residual after laser-clot ablation. It must also be noticed that even at higher values the produced temperature should be less than the material (PLGA or CS) melting temperature which was so in our case.

For example, the weight of digested clot percent after laser exposure is 33.27% for photomechanical drug delivery compare with 21.6% for drug delivery in group PLGA/CS NPs, 31.13% for photomechanical drug delivery compare with 15.54% for drug delivery in group PLGA NPs and 17% for photomechanical drug delivery compare with 8.05% for drug delivery in group tPA only. The results show that the PLGA/CS NPs maintain the highest weight percentages of dissolved clot.

Table 4. laser thrombolysis of clot after exposure to NPs (after 1 hr).

Sample	Initial weight (mg)	Final weight (mg) After laser exposure	Weight of digested clot (%)
tPA only	100	83	17
tPA-PLGA NPs	299.3	206.1	31.13
tPA-PLGA/CS NPs	316.2	211	33.27

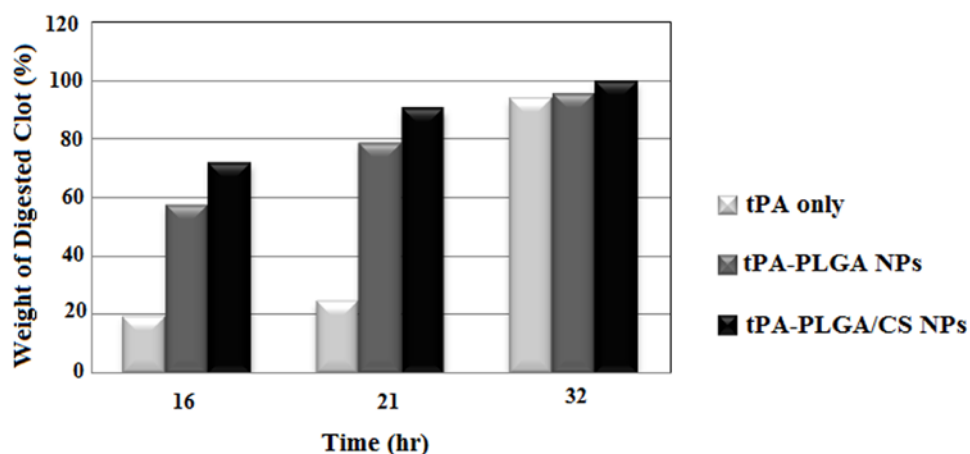


Fig.13. The weight of digest clot percent after laser exposure with $F=109 \text{ Jcm}^{-2}$ at different times.

4. Discussion

PLGA particulate drug delivery systems have been widely used for biomacromolecules such as peptides, proteins or nucleic acids [39,40]. In this study, the tPA encapsulated PLGA and PLGA/CS were fabricated by double emulsion solvent evaporation (W/O/W). Sustained and localized release, as well as *in vivo* stabilization can be achieved using PLGA particles. However, during preparation, organic solvents and shear stress can denature or deactivate the biopolymers incorporated. The EE* of biopolymers in the particles is essentially low and results in the consumption of a large quantity of biopolymers in the preparation [41]. Hence surface coating of PLGA particles seems to be useful in reducing their effect.

In this report, CS was used to coat PLGA NPs due to their cationic charge, biodegradability and mucoadhesive properties. In addition, CS coated PLGA NPs have been proposed for delivery of protein drugs. CS has been shown to possess mucoadhesive properties due to molecular attractive force formed by electrostatic interaction between positively charged CS and negatively charged surfaces. These properties may be attributed to: (1) strong hydrogen bonding groups like -OH, -COOH, (2) strong charges, (3) high molecular weight, (4) sufficient chain flexibility, and (5) surface energy properties. The electrostatic attraction is likely the predominant driving force especially in the formation of the first monomolecular adsorption layer [41]. The adsorption of CS continues even though a positively charged surface has been achieved, in which hydrogen bond (N-H) or van der waal's force can be involved. At high concentration of CS, it is possible that the subsequent layer of CS could be adsorbed on the first layer and has no direct contact with the surface. With more layers added, CS chains would repel each other due to the same charge but be attracted and interact through hydrophobic interactions, van der waal's forces and hydrogen bonds [31,41].

The reasons for encapsulating tPA as the thrombolytic drug are due to: i- the extremely short half life (<5min) renders the need for administering a high dose (1.25 mg/kg) of tPA. However, the effective therapeutic dose range of tPA at the thrombus site is only around 0.45-1 $\mu\text{g/ml}$ [42]. ii- due to administration of this high dose, clinical use of tPA is often associated with a high incidence of bleeding complication, and iii- in order to prevent restenosis for up to several months, prolonged attenuation of thrombus by utilizing a delivery carrier for thrombolytic drug has been suggested. CS was chosen as coating on the surface PLGA for encapsulation of tPA, mainly because zeta potential of fibrinogen solution is -38.5 at pH of 7.4 [23]. Hence, it would be reasonable to postulate that the zeta potentials of fibrins in blood clots have negative charge and that may facilitate the penetration of the NPs into clots.

Morphology and spherical shape of NPs is shown by TEM micrographs and AFM images and is shown size of the tPA encapsulated PLGA/CS NPs is larger than PLGA NPs. The hydrodynamic diameter of CS coated PLGA NPs increases gradually with initial CS

concentration. The increased particle size can be attributed to the increased viscosity of CS and the increased amount of adsorbed CS on the surface of PLGA NPs.

The positive zeta potential and FTIR spectroscopy (Fig.5) of CS coated PLGA NPs confirmed the presence of CS on PLGA NPs. Guo and et al. [41] reported that continuous adsorption of CS on PLGA NPs do not affect the apparent zeta potential at high concentration (greater than 0.4-0.6 g/l). The zeta potential with increases initial CS can be indicative of saturated adsorption of CS on PLGA NPs. However, the amount of adsorbed CS on PLGA NPs increases with the initial CS concentration and saturation of adsorption. The small size and the high surface energy of PLGA NPs play an important role for multilayer adsorption of CS [41]. The increase of NPs size and the spectra of NPs with peaks at 1629, 2923, 2853 and 3431 cm^{-1} confirm the formation of the CS (Fig.5b) on the PLGA NPs surface.

The DSC curves of PLGA NPs (Fig.6e) and PLGA/CS NPs (Fig.6f) correspond to relaxation enthalpy of pure PLGA (55°C). It can be observed that the nanoencapsulation process did not affect the polymer structure because the pure PLGA presented the same value for relaxation enthalpy. The DSC study did not detect any drug material in the NPs i.e. the endothermic peak of tPA was not observed. Thus, it can be concluded that the drug incorporated into the NPs was in an amorphous polymer. The thermal decomposition of PLGA NPs and PLGA/CS NPs has begun in a lower temperature than that of the pure PLGA and CS. The nanoparticles are more exposed to the thermal degradation because their sub-micrometric size makes the superficial area larger. In relation to polymer, since NPs show wider superficial area they degrade easier. They were not observed peaks in approximately 355 °C and 300 °C, that seem to be characteristic of pure PLGA and CS (curve b and c Fig.6), confirming the previous data that show PLGA NPs and PLGA/CS NPs to have lower thermal stability than pure PLGA and CS. The thermal decomposition of PLGA/CS NPs is lower than thermal decomposition of PLGA NPs. The coating of NPs with CS makes the superficial area larger and show wider superficial area they degrade easier. The PLGA/CS is more reactive than the pure polymers due to their wider superficial area and, consequently, they suffer thermal decomposition more quickly.

EE* of PLGA/CS NPs was higher compared with PLGA NPs. Effect of coating with CS on loading efficiency might be caused by an ionic interaction between tPA and CS and prevented leakage of tPA from emulsion droplet during evaporation process. The drug release of PLGA and PLGA/CS NPs were monitored during the first hour of release which accounted for 11% and 7.8 % respectively. This difference is explained by the fact that it takes some times for CS to degrade and let tPA to diffuse out as well as the fact that higher hydrodynamic pressure is experienced in the opposite direction (i.e. acting as resistance). However, after this short time some degradation and PBS uptake is taken place as a result of which the release trend gradually increases. Longer drug release time due to the diffusion process is much slower compared with the initial release. Several concurrent processes such as interactions between tPA and CS and between CS and PLGA, most probably influence the release of tPA. Therefore, depending on the ratios of the different components in each particle type, the influence of the increased CS solubility in acidic media (pH=5) on the release of the drug, is not directly proportional to the CS content of each NPs. Faster release from the PLGA/CS NPs in media is attributed to the higher solubility of CS at lower pH [43]. The final stage was the release of drug for few days where the process was completed. The complete release of the drug from the NPs occurred only after complete erosion or degradation of the NPs. Sustained release of tPA is sufficient to prevent the formation of new thrombus. In order to prevent restenosis for up to several months, the tPA should be release in controlled manner for longer period of time. Indeed, several researches have indicated a lower rate of restenosis using a local infusion of tPA [44-45]. Therefore, our studies could offer an alternative for currently existing antithrombotic therapies.

Efficient thrombolysis appears to be dependent upon transport of the tPA into clot, which is a function of both diffusion and convection. The tPA incorporated in the NPs retained its activity, as confirmed by the fibrin clot lysis assay (Fig.11). The weight percentage of dissolved clots is shown in the following order, PLGA/CS NPs (21.6%) > PLGA NPs (15.54%) > tPA (8.05%). The highest dissolved clot rate was obtained with PLGA/CS NPs, suggesting the effect and importance of the interaction between the CS and blood clot. Therefore, PLGA/CS NPs could

serve as an effective vehicle for local delivery of tPA in an attempt to alleviate the systemic side effects of the drug and to enhance its efficacy in thrombolytic therapy.

Laser thrombolysis is another method of optomechanical removal of clot that is currently under investigation. The goal of laser thrombolysis is to safely obliterate the embolus into microscopic fragments small enough to pass through the capillary circulation. Laser thrombolysis for acute stroke uses a low laser energy pulse of laser tuned to the hemoglobin absorption peak or facilitated by an exogenous administered chromophore. The absorbed energy vaporizes the hemoglobin molecule and adjacent water molecules to create a vapor bubble that expands and contracts to create shock waves that focally shatter the embolus [46]. Our demonstrate the possibility of using photomechanical drug delivery (compare with drug delivery) to enhance the thrombolysis process by delivering nanoparticles into clot during the laser irradiation and possibly to remove the clot residual after initial laser-clot ablation.

Since 532nm laser pulse is absorbed more efficiently by blood clot than by the surrounding arterial wall, thus, that the clot can be heated and vaporized without damaging adjacent structures and reducing the chance of a new clot forming. Avoiding damage to the arterial wall is also important in the prevention of re-stenosis, or renewed narrowing. This demonstrates that a 532 laser pulse can enhance delivering of tPA into clot. The main operating mechanism with this laser in an absorbing liquid media such as blood is due to rapid generation of acoustic waves via thermoelastic mechanism and vaporization (photothermal). Further, the rapid breakdown and plasma formation cause heating of a small volume of liquid around the focus of a converging lens leads to the formation of a body of high-temperature vapour called a cavitation bubble (photomechanical). Most explanations have focused on cavitation-related processes such as microstreaming around the bubbles in stable cavitation, or microjetting in unstable cavitation, both of which can alter the structure of clots. In all cases, microbubbles may also increase the number of available binding sites for fibrinolytic enzyme molecules by stretching or damaging clot fibers. Therefore, nanoparticles are likely driven into the clot by thermomechanical waves (ultrasonics) at low fluencies and also by hydrodynamic flow due to the cavitation microbubble formation at higher values. These results suggest that PLGA/CS NPs could serve as an effective vehicle for local delivery of tPA in cardiological applications.

5. Conclusions

The PLGA-encapsulated tPA NPs and the CS-coated PLGA-encapsulated tPA (PLGA/CS) NPs have been synthesized by W/O/W method. The EE* and size of NPs was increased by coating with CS. *In vitro* drug release experiments showed a sustained release profile for 3 days. Therefore, sustained release of tPA is sufficient to prevent the formation of new thrombus. In order to prevent restenosis for up to several months, the tPA should be released in a controlled manner for longer period of time. The PLGA/CS NPs successfully thrombolysed the clot-occluded tube and showed the highest percentages of clot weight loss. Encapsulation of tPA in PLGA/CS has important effects, including acting as a shield to protect the drug from inactivation and increasing its half-life. Also, higher drug circulation in time allows the administration of a lower dosage, with decreased probability of side-effects. In addition, encapsulation helps to avoid bleeding complication. The DSC curves confirmed reinforcing the idea that the drug was entrapped in the NPs. Also, this study demonstrated the thrombolysis process can be enhanced by delivering tPA into clot by laser pulse. The weight percentages of dissolved clot was higher for photomechanical drug delivery method than using normal drug delivery method (ie. without laser), indication a deeper penetration of particles within the clot tissue bulk. It must also be noticed that even at higher values the produced temperature should be less than the material (PLGA or CS) melting temperature which was so in our case. The results of this report suggest that the NPs could potentially be used as carrier for local delivery of a thrombolytic drug and the PLGA/CS NPs maintain the highest weight percentages of dissolved clot. Therefore, photomechanical drug delivery using PLGA/CS NPs may be employed in future clinical studies.

Acknowledgment

The authors would like to thank the Novel Drug Delivery Systems Lab and Pharmaceutical Science Research Center of Tehran University for their collaboration.

References

- [1] A. S. Buteica, D. I. Mihaiescu, A. M. Grumazescu, B. S. Vasile, et al., *Digest J. of Nanomat. and Biostructure*, **5**, 927 (2010).
- [2] Y. N. Konan, R. Gruny, E. Allemann, *J. photochem. Photobiol. B* **66**, 89 (2002).
- [3] R. Pjanović, N. B. Vragolović, J. V. Giga, R. G. Grulović, B. Bugarski, *J. of Chem. Techno. and Biotech.* **85**, 693 (2010).
- [4] J. E. Riviere, M. C. Heit, *Pharm. Res.* **14**(6), 687 (1997).
- [5] K. Tachibana, S. Tachibana, *Jpn J. Phys.* **38**, 3014 (1999).
- [6] S. Gambihler, M. Delius, J. W. Ellwart, *Naturwissenschaften* **79**(7), 328 (1992).
- [7] T. Kodama, Y. Tomita, *Appl. Phys. B* **70**, 139 (2000).
- [8] M. Ogura, S. Sato, M. Terakawa, H. Wakisaka, M. Uenoyama, et al., *Jpn J. Appl. Phys.* **42**, L977 (2003).
- [9] J.K. Leach, E. Patterson, E.A. Orear, *J. of Thrombosis and Haemostasis* **2**, 1548 (2004).
- [10] H.Q. Shangguan, K.W. Gregory, L.W. Casperson, S.A. Prael, *Laser Surg. Med.* **23**(3), 151 (1998).
- [11] H. Yamamoto, Y. Juno, *J. Contrl. Release* **102**, 173 (2005).
- [12] H. Q. Mao, K. Roy, V. L. Troung-Le, K. A. Janes, *J. Contrl. Release* **70**, 399 (2001).
- [13] Y. Xu, Y. Du, *Interna. J. of Pharma.* **250**, 215 (2003).
- [14] R. P. Lanza, R. Langer, J. Vancanti, J., Editors. *Principles of tissue engineering*. 2nd, Academic Press, San Diego (2000).
- [15] T. W. Chung, Y. F. Lu, S. S. Wang, Y. S. Lin, S. H. Chu, *Biomaterials* **23**, 4803 (2002).
- [16] K. Tahara, T. Sakai, H. Yamamoto, H. Takeuch, Y. Kawashima, *Interna. J. of Pharma.* **354**, 210 (2008).
- [17] J. W. Welsel, J. P. Collet, *J. of Thrombosis and Heamostasis* **2**, 1545 (2004).
- [18] J. K. Leach, E. Patterson, E. A. Orear, *J. of Thrombosis and Heamostasis* **2**, 1548 (2004).
- [19] J. K. Leach, E. Patterson, E. A. Orear, *Thromb. Heamost.* **91**, 1213 (2004).
- [20] Y. Xie, M. Kaminski, M. D. Torno, *J. of Magnetism and Magnetic Material.* **311**, 376 (2007).
- [21] P. D. Nguyen, E. A. Orear, A. E. Johnson, E. Patterson, *Circulation Research* **66**(3), 875 (1990).
- [22] M.J. Heslinga, E.M. Mastria, O.E. Adefeso, *J. Contrl. Release* **38**, 235 (2009).
- [23] T.W. Chung, S.S. Wang, W.J. Tsai, *Biomaterials* **29**, 228 (2008).
- [24] H. Nazari, M. Jafari, *Digest J. of Nanomat. and Biostructure* **5**, 909 (2010).
- [25] Z.L. Li, N.Z. Zhang, Y.H. Nie, *Chung Hual Hseeh Tsa Chih* **74**, 338 (1994).
- [26] J.L.M. Heeremans, R. Prevost, M.E.K. Bekkers, et al, *Throm Haemos.* **73**, 488 (1995).
- [27] J.K. Leach, E.A. Orear, E. Patterson, Y. Miao, A.E. Johnson, *Throm Haemost.* **90**, 64 (2003).
- [28] F. Esmaeili, F. Atyabi, R. Dinarvand, *J. of Exprimental Nanoscience* **2** (3), 183 (2007).
- [29] R. Dinarvand, S. H. Moghadam, A. Sheikhi, F. Atyabi, *J. of Microencapsulation* **22**(2), 139 (2005).
- [30] S. Shrivastava, *Digest J. of Nanomat. and Biostructure* **3**, 251 (2008).
- [31] V. R. Sinha, A. K. Singla, S. Wadhawan, R. Kaushik, R. Kumria, K. Bansal, S. Dhawan, *Inte. J. of Pharm.* **274**, 1 (2004).
- [32] W. Zheng, *Interna. J. of Pharma.* **374**, 90 (2009).
- [33] T. Hino, Y. Kawashima, S. Shimabayashi, *Advanced Drug Delivery Reviews* **45**, 27 (2000).
- [34] T. Higuchi, *J. Pharmaceut Sci.* **52**, 1145 (1963).
- [35] M. C. Gohel, M. K. Panchal, V. V. Jogani, *AAPS Pharm.Sci.Tech.* **1**(4), article 31(2000),
- [36] P. Riger, N. A. Peppas, *J. Control.Release* **5**, 23 (1987).

- [37] P. Cintas, F. Nguyen, B. Bonen, V. Larrue, *J. of Thrombosis and Haemostasis* **2**, 1163 (2004).
- [38] Q. Xu, J.T. Czernuszka, *J. Contrl. Release* **127**, 146 (2008).
- [39] E. Cohen-Sela, M. Chorny, N. Koroukhov, H.D. Danenberg, G. Golomb, *J. Control Release* **127**, 146 (2008).
- [40] H.Takeuchi, H. Yamamoto, Y. Kawashima, *Adv. Drug Delivery Review* **47(1)**, 39 (2001).
- [41] C. Guo, R.A. Gemeinhart, *European J. of Pharma. and Biopharma.***70**, 597 (2008).
- [42] Y. J. Park, J. Liang, Z. Yang, V. C. Yang, *J. of Controlled Release* **75**, 37 (2001).
- [43] M. L. Manca, G. Loy, M. Zaru, S. G. Antimisiaris, *Colloids and Surfaces B: Biointerfaces* **67**, 166 (2008).
- [44] K. Kanamasa, N. Ishida, H. Kato, S. Sakamoto, *Circulation* **90**:1185 (1995).
- [45] J. Gellman, S. L. Sigal, Q. Chen, *J. Am. Coll. Cardiol.* **17**, 25A (1991).
- [46] G.M. Nesbit, G. Luh, R. Tien, S.L. Barnwell, *J. Vasc Interv Radiol.* **15**, S103 (2004).